

# Infection Biology of *Moniliophthora perniciosa* on *Theobroma cacao* and Alternate Solanaceous Hosts

Jean-Philippe Marelli · Siela N. Maximova ·  
Karina P. Gramacho · Seogchan Kang ·  
Mark John Gultinan

Received: 27 May 2009 / Accepted: 13 November 2009 / Published online: 21 November 2009  
© Springer Science + Business Media, LLC 2009

**Abstract** The C-biotype of *Moniliophthora perniciosa* is the causal agent of witches' broom disease of *Theobroma cacao* L. While this disease is of major economic importance, the pathogenicity mechanisms and plant responses underlying the disease are difficult to study given the cacao tree's long life cycle and the limited availability of genetic and genomic resources for this system. The S-biotype of *M. perniciosa* infects solanaceous hosts, particularly pepper (*Capsicum annuum*) and tomato (*Solanum lycopersicum*). These species are much more amenable for performing studies of mechanisms underpinning host-pathogen interactions as compared to cacao. A phylogenetic analysis performed in this study demonstrated that S-biotype strains clustered with C-biotype strains, indicating that these biotypes are not genetically distinct. A comparative analysis

demonstrated that disease progression in tomato infected with the S- biotype is similar to that described for cacao infected with the C- biotype. The major symptoms observed in both systems are swelling of the infected shoots and activation and proliferation of axillary meristems. Cellular changes observed in infected tissues correspond to an increase in cell size and numbers of xylem vessels and phloem parenchyma along the infected stem. Observations revealed that fungal colonization is biotrophic during the first phase of infection, with appearance of calcium oxalate crystals in close association with hyphal growth. In summary, despite different host specificity, both biotypes of *M. perniciosa* exhibit similar disease-related characteristics, indicating a degree of conservation of pathogenicity mechanisms between the two biotypes.

**Keywords** *Moniliophthora perniciosa* · *Theobroma cacao* L. · *Solanum lycopersicum* · *Capsicum annuum* · Fungal pathogenicity · Plant defense

---

Communicated by: Schuyler S. Korban

J.-P. Marelli · S. Kang  
Department of Plant Pathology,  
The Pennsylvania State University,  
Buckhout Lab,  
16802 University Park, PA, USA

S. N. Maximova · M. J. Gultinan (✉)  
Department of Horticulture, The Pennsylvania State University,  
422 Life Sciences Building,  
16802 University Park, PA, USA  
e-mail: mjpg9@psu.edu

K. P. Gramacho  
CEPLAC/CEPEC/SEFIT,  
Caixa postal 07 45600-000 Itabuna, Bahia, Brazil

*Present Address:*

J.-P. Marelli  
Mars Center for Cocoa Science,  
Caixa postal 55 45630-000 Itajuípe, Bahia, Brazil

## Introduction

*Moniliophthora* (= *Crinipellis*) *perniciosa* (Stahel) Sing., is a basidiomycete fungus [2], closely related to the common button mushroom *Agaricus bisporus* [36]. The fungus is a pathogen of *Theobroma cacao* L., the chocolate tree, and the disease's common name, witches' broom, is due to the appearance of dried and distorted shoots on the infected trees [44]. *Moniliophthora perniciosa* is indigenous to the Amazon basin region in association with several plant species in the genus *Theobroma* (Malvaceae) and also in plants from families unrelated to the Malvaceae [4]. Multiple biotypes of *M. perniciosa* are defined based on host adaptation: C-biotype infecting *T. cacao*; L- biotype

associated with members of the Bignoniaceae [19]; H-biotype that can infect members of the Malpighiaceae and S-biotype associated with members of the Solanaceae [5]. Based on morphological and molecular data, the H-biotype was reclassified to a new species, *Crinipellis brasiliensis* [9]. The S-biotype was originally discovered on *Solanum rugosum* and *Solanum lasiantherum*, both solanaceous weeds present near cocoa farms in the Amazon [5]. Infection with S-biotype basidiospores of cultivated solanaceous like *Solanum lycopersicum* (tomato) and *Capsicum annuum* (pepper) in greenhouse conditions, induced stem swelling and hypertrophied buds [5]. However, in nature, *M. perniciosa* is not epidemic on cultivated solanaceous, indicating that the annual life style of these crops is not conducive for the full completion of the pathogen life cycle [14]. Cross infectivity between the C- and S-biotypes has not been observed under controlled experiments but, morphological and genetic evidence suggests that these biotypes belong to a single species [9, 20].

In nature, basidiospores of *M. perniciosa*, are the only known infectious propagules, germinating on young cacao tissues such as apical and axillary meristems, young leaves, developing flowers, and fruits [30, 36], and subsequently penetrating plant tissues directly or entering through stomata [15, 43]. The pathogen exhibits two phases in its disease cycle, the biotrophic phase and the necrotrophic phase. Germinated basidiospores form a swollen (5–20  $\mu\text{m}$ ) monokaryotic hyphae that grows intercellularly as a biotroph [13] and causes symptoms that include shoot swelling, petiole swelling, and loss of apical dominance [30]. The biotrophic phase usually lasts for about 60 days in artificially inoculated plants [40]. In the necrotrophic phase of infection, from the apex downwards, the green broom becomes brown and dies within a week [30, 42]. This phase is associated with the appearance of intra-cellular hyphae, which is dikaryotic and exhibits clamp connections [37]. When the dried broom is exposed to alternate periods of dry and wet weather, basidiocarps emerge to complete the life cycle [34].

A witches' broom epidemic recently occurred in 1989 in Bahia, Brazil, which was once the second most productive cacao-producing region in the world. In the subsequent ten years, cocoa bean production in this region has declined from 300,000 tons to 130,000 tons causing a loss of \$235 million annually and socioeconomic hardship in the region [6, 30]. The development of effective control measures against *M. perniciosa* is one of the major challenges in boosting cacao production in South America. Equally critical is avoiding the introduction of the pathogen to Africa and Asia where the disease has not yet been observed. A better understanding of the physiological and genetic mechanisms underpinning the development of this disease is vital for protecting global cacao production from

witches' broom. However, research on *M. perniciosa*/*T. cacao* interactions has been difficult because of cacao's slow and long life cycle, irreproducible infection efficiencies under laboratory conditions, very limited genetic/genomic resources, and the complexity of *M. perniciosa*'s disease cycle [8, 12].

To address this problem, this study aimed to use the S-biotype of *M. perniciosa* on cultivated solanaceous. Because *Solanum lycopersicum* (tomato), in particular, has been extensively used as a model plant for basic biological research, many molecular and genetic tools are available and can be used to elucidate some of the questions remaining on the effect of this pathogen on the plant's physiology.

As the first step of this study, phylogenetic relationships, colonization patterns, and the disease cycles of the S and C biotypes, were investigated. Cellular mechanisms underlying the development of the typical symptoms of the biotrophic phase (stem swelling and release of axillary buds) were also studied via morphometric analyses of the affected areas. Lastly, utilizing transgenic tomato plants harboring an auxin responsive reporter gene (DR5-GUS auxin responsive promoter), changes of this hormone occurring during infection, were monitored.

## Results

### Symptomology in Cacao, Pepper, and Tomato

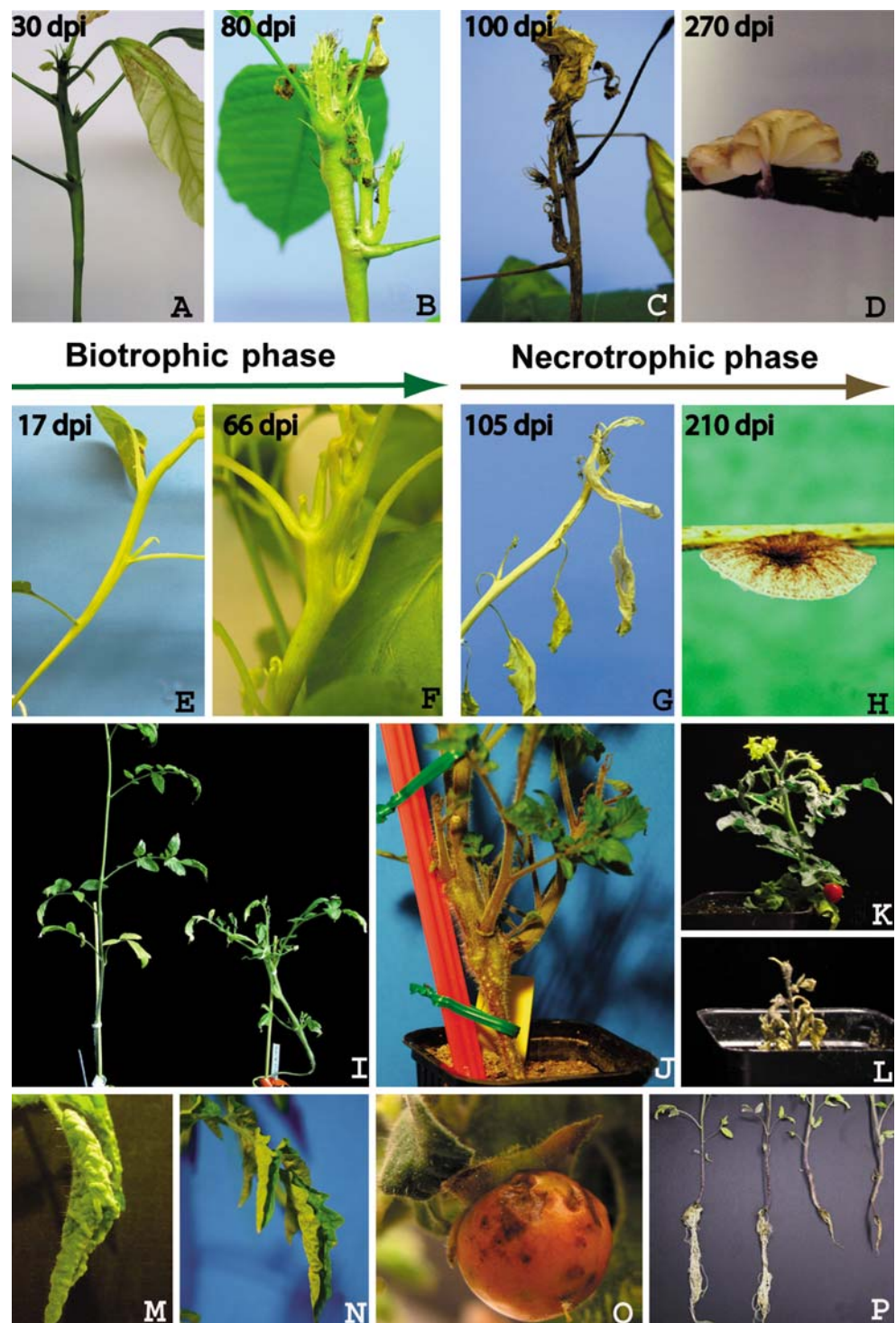
As previously described [42], infected cacao plants exhibited the first symptom of infection about 30 days post inoculation (dpi), in the form of a slight swelling of the stems (Fig. 1a). Activation of axillary meristems and swelling near the infection point was observed during later stages of infection during the biotrophic phase of the disease (Fig. 1b).

The developmental switch from the biotrophic to the necrotrophic phase of infection occurred at about 100 dpi, causing a total necrosis of the shoot within 2–3 days (Fig. 1c). Exposing the dried shoot to conditions conducive for sporulation caused basidiocarps to form on the dry branches within 270 dpi (Fig. 1d).

The pepper variety, Tequila Sunrise, was used for verifying the pathogenicity of S-biotype strain 73-6-01 (Fig. 1e to h). Witches' broom symptoms (stem swelling and activation of the axillary meristems) were recorded at 17 dpi (Fig. 1e). The biotrophic phase lasted up to 90 dpi in pepper (Fig. 1f) Total necrosis of the infected shoot was observed at 105 dpi, but the progression was slower than in cacao (Fig. 1g). When the dry shoot was exposed to sporulation conditions, basidiocarps appeared at 210 dpi (Fig. 1h).

The same general progression of symptoms was also observed in tomato plants inoculated with S-biotype strain

**Fig. 1** Symptoms observed in cacao plants (a–d) and pepper (e–h) infected with *M. perniciosa*. The biotrophic phase in *S. lycopersicon*; **i** left uninoculated plant, right, inoculated plant that expresses swelling, activation of axillary buds and stunting. **j** Stem swelling and activation of meristems on an infected plant. **l** The necrotrophic phase in Micro-Tom compared to (**k**) a non-inoculated plant bearing fruits and flowers. **m** Blisters on leaves of an infected plant. **n** Leaf curling in an infected plant. **o** Necrosis of the pericarp on tomato fruits of Micro-tom. **p** Root atrophy in infected tomato plants



73-6-01, with a few differences (Fig. 1i–p). First, the transition to the necrotrophic phase was not observed in the tomato variety NC841.73 under the same growing conditions (Fig. 1i and j) whereas the tomato variety Micro-Tom did transition to the necrotrophic phase within one month (Fig. 1k and l). Second, in addition to the expected stem swelling and activation of axillary meristems (Fig. 1j), infected tomato plants developed additional symptoms not

observed on cacao or pepper plants. About 15 dpi, NC841.73 plants developed blisters along leaf veins (Fig. 1m). Inspection of these blisters under microscopy revealed that they consisted of an enlarged dedifferentiated group of cells resembling callus.

Additional symptoms included leaf curling (Fig. 1n), fruit necrosis on Micro-Tom (Fig. 1o), and hypertrophy of the root system (Fig. 1p).

## Phylogenetic Analysis of Strains of the C and S Biotypes of *M. perniciosa*

The resulting phylogenetic tree consists of three well-resolved groups (Fig. 2). The first group included all isolates of *M. perniciosa* collected from cacao, pepper, solanaceous hosts (*S. paniculatum*, *S. lycocarpum*, *S. rugorosum*) and cacao relatives (*T. grandiflorum*, *T. subincanum* and *Herrania*). Some S-biotype isolates (Jurubeba06, 73-6-01, CP37 and 92-10-7) appeared to cluster, but the bootstrap support for this subgroup (39%, Fig. 2) was weak. The second group contained two strains of *M. roreri* (na\_M.roreri, and Mgflorum), supporting the proposed divergence from the first group. The third group was represented by strain CBB361 of *Marasmius* spp. (the outgroup).

## Cellular Changes Underlying Symptoms in Tomato Plants Colonized with *M. perniciosa*

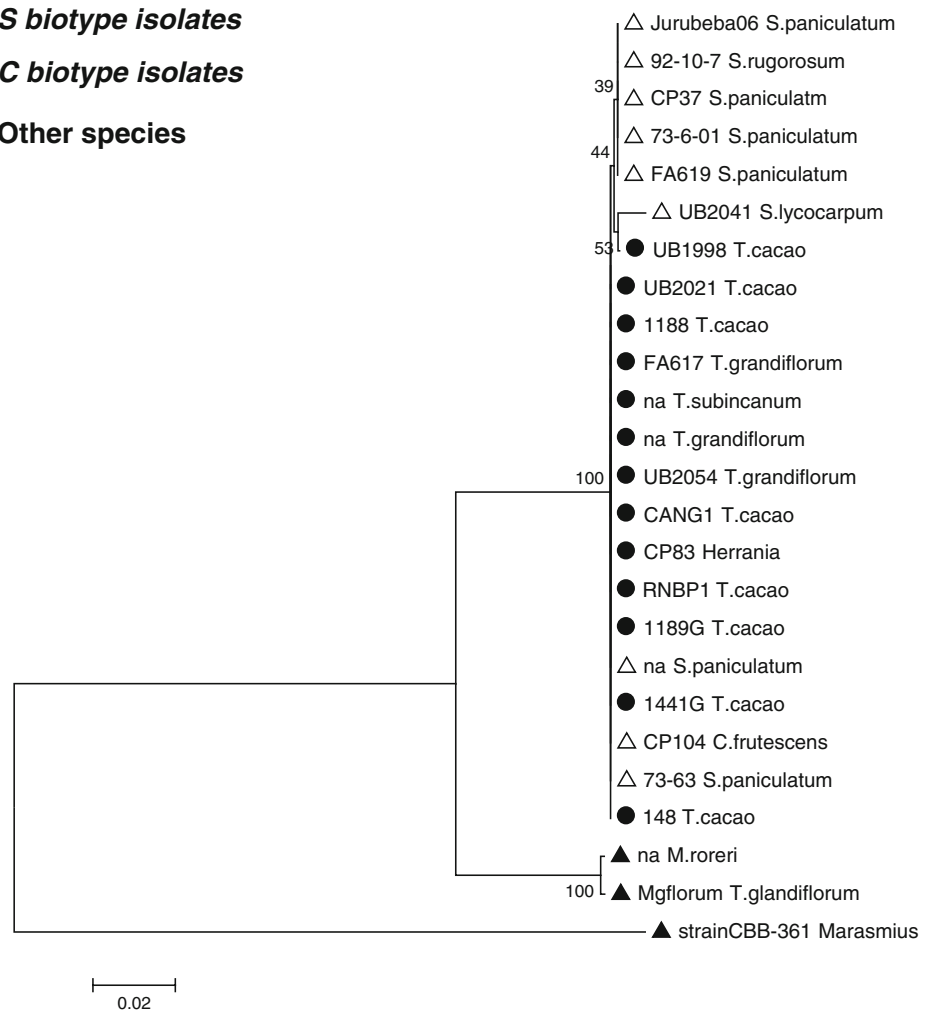
Comparison between tissue areas in the calcofluor stained cross sections of infected and control stems showed that the

total area of cortex, phloem, xylem and pith in infected shoots was unquestionably higher (Fig. 3a and b). The most significant difference between control and infected plants appeared at positions Hyp (Hypocotyl) and Cot (Cotyledons) (Fig. 3c). At the Hyp position, the phloem and xylem areas were 14 and 10 times larger respectively in infected plants compared to controls. At the Cot position, the phloem and xylem areas were 7 and 5 times larger respectively, on infected plants compared to controls. On more distal positions of the plant shoot (1st, 2nd and 4th internode); this difference was attenuated for phloem and xylem. The cortex was between 2 and 5 times larger in infected plants compared to controls (Fig. 3c). The pith was only one to two times larger in the infected tissues compared to the control tissues, except in the fourth internode where it became 5 times larger in infected tissues (Fig. 3c).

A more detailed quantification was performed by counting the number of cells and the average cell size in the most affected tissues (phloem and xylem). In phloem, the total number of cells in infected plants was significantly higher than in the uninfected control plants at all positions

**Fig. 2** Phylogenetic tree based on DNA sequences of the ITS regions (ITS1, 5.8S RNA, and ITS2) from isolates of *Moniliophthora* spp., *M. roreri* and *Marasmius* spp. (CBB361). The symbol preceding each strain name indicates the biotype (as indicated in the key on the left side of the picture). The numbers above the branches indicate the bootstrapping support. The tree was generated by neighbor joining analysis using MEGA 3.1, and statistical support for branch topology was tested by bootstrap analysis derived from 1000 replicates

- △ **S biotype isolates**
- **C biotype isolates**
- ▲ **Other species**



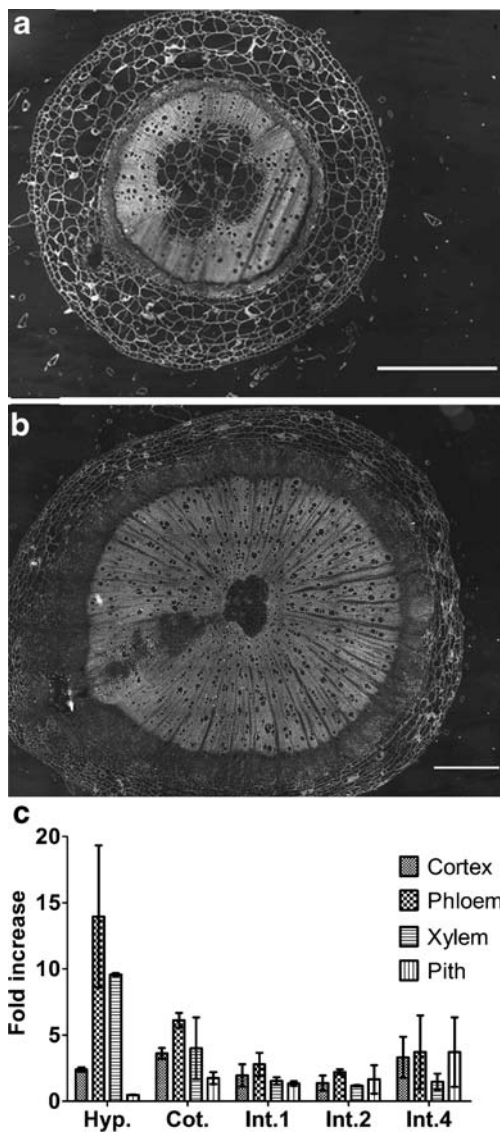


**Fig. 3** Cellular changes induced by *M. perniciosa* infection in tomato. Photomicrographs of stem cross sections at the hypocotyl position in non-infected (a) and infected (b) plants (Bar=1000 $\mu$ m) are shown. c The total fold increase in tissue area compared to the controls, measured at five different sections along the plant stem, Hypocotyls (Hyp.), Cotyledon node (Cot.), first internode (Int.1), second internode (Int.2) and fourth internode (Int.4) are shown

(Fig. 4a). At the hypocotyls (H) position, 10 times as many cells appeared as in the control plants, whereas at the 4th internode, only a 1.5 fold increase occurred (Fig. 4a). Because cell size in the tissues varied substantially, the cell size distributions between control and infected plants at five positions (Fig. 4b, c, d, and f). The distribution significantly shifted toward larger cells in the stems of infected plants compared to uninfected control plants (Fig. 4b, c, d, and f). Those differences were attenuated at the 4th internode, where the distributions, although still different, overlapped (Fig. 4f).

In the xylem, clear differences between infected and control plants also appeared (Fig. 5). The total number of cells was significantly higher at four positions H, C, 1 and 2 (Fig. 5a). However, at position 4 no significant differences in cell numbers were observed (Fig. 5a). Similar to the phloem, the cell size distribution also significantly shifted toward higher values in infected plants (Fig. 5b, c, d, e, and f). However, the distributions of the control and infected plants overlap when measurements were made at the 4th internode (Fig. 5f).

#### Fungal Colonization and Pathogenicity

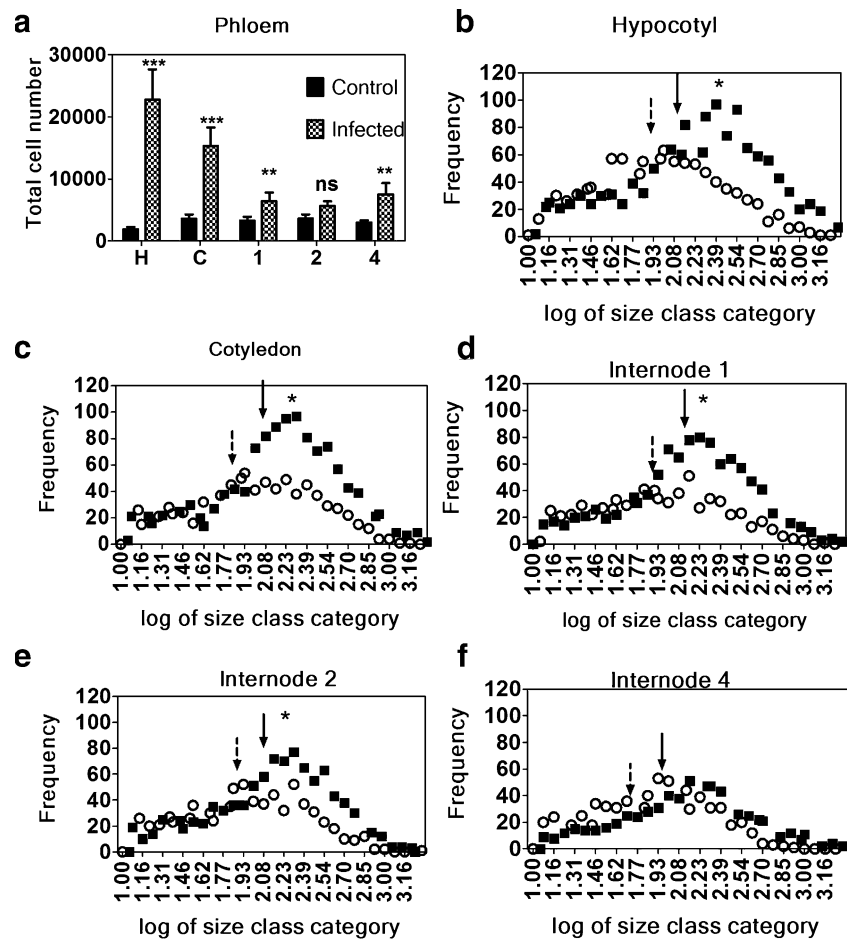
In DR5-GUS transgenic Micro-Tom, carrying an auxin responsive promoter-reporter gene, a clear difference in the levels of GUS expression between infected and control plants appeared (Fig. 6a and b). Uninfected DR5-GUS control plants had a low expression of GUS near the primary xylem (Fig. 6a) while infected plants exhibited a higher GUS staining in the primary xylem which correlated with the zone of stem swelling, increased cell enlargement and numbers as described earlier (Fig. 6b). This increased staining was reproducible in at least 2 different transgenic lines.

Septate biotrophic hyphae grew intercellularly, predominantly associated with phloem parenchyma cells, but did not appear to colonize the plant extensively (Fig. 6c). Intercellular crystals were often co-localized with hyphae in the apoplastic space (Fig. 6c). Using the polarized light method and chemical staining with silver nitrate [28], these crystals were identified as calcium oxalate ( $\text{CaC}_2\text{O}_4$ ).

#### Discussion

To compare and contrast the similarities of the infection biology of *M. perniciosa* between solanaceous hosts and cacao the genetic relationship between the C- and S-biotypes was investigated, and morphological/cellular analyses during disease progression were conducted in tomato and pepper. Isolates of *M. perniciosa* from solanaceous hosts were found to belong to the same phylogenetic group as those collected from *T. cacao* or its relatives, *T. grandiflorum*, *T. subincantum*, and *Herrania* sp. A similar study, which used ITS sequences to compare isolates of the C, S, and H biotypes of *M. perniciosa*, reported that whereas the S- and C- biotypes grouped in the same phylogenetic clade, the H-biotype isolate collected from *H. acutifolia* formed a different species and was renamed to *Crinipellis brasiliensis* (based on the previous name, *Crinipellis perniciosa*) [9]. In another study involving isolates of the C and S biotypes, the numbers of chromosomes varied considerably among strains, but no correlation between karyotypes and host specificity could be

**Fig. 4** Cellular changes induced by *M. perniciosa* infection on tomato phloem. Cell number between infected and control plants at 5 different positions (C=cotyledons, H=hypocotyls, 1,2 and 4=first, second and fourth internode). Mean values were compared using a student t-test (a). Distributions of cell sizes using a logarithmic transformation (b–f). The distributions were compared using a Mann-Whitney test. The mean size values of the cell size for control (dashed arrows) and infected (solid arrows) are shown with an asterisk when differences are statistically significant



established [38]. Based on AFLP and RAPD analyses, the S-biotype formed a distinct group from the C-biotype [3, 35]. However, in both studies only one or two isolates of the S-biotype were included. In contrast, in this study nine isolates of S-biotype strains collected from four different solanaceous hosts were characterized. The clustering pattern between S- and C-biotype isolates suggests that these biotypes are not genetically distinct. In previous studies, cross inoculations performed on cacao and tomato using both S- and C-biotypes, only the S-biotype could induce symptoms on tomato and only the C-biotype could induce symptoms on cacao [5]. This suggests that host specificity in *M. perniciosa* could be determined by a complex recognition system that is not yet known. The available genome sequence [31] will allow studies to understand such question.

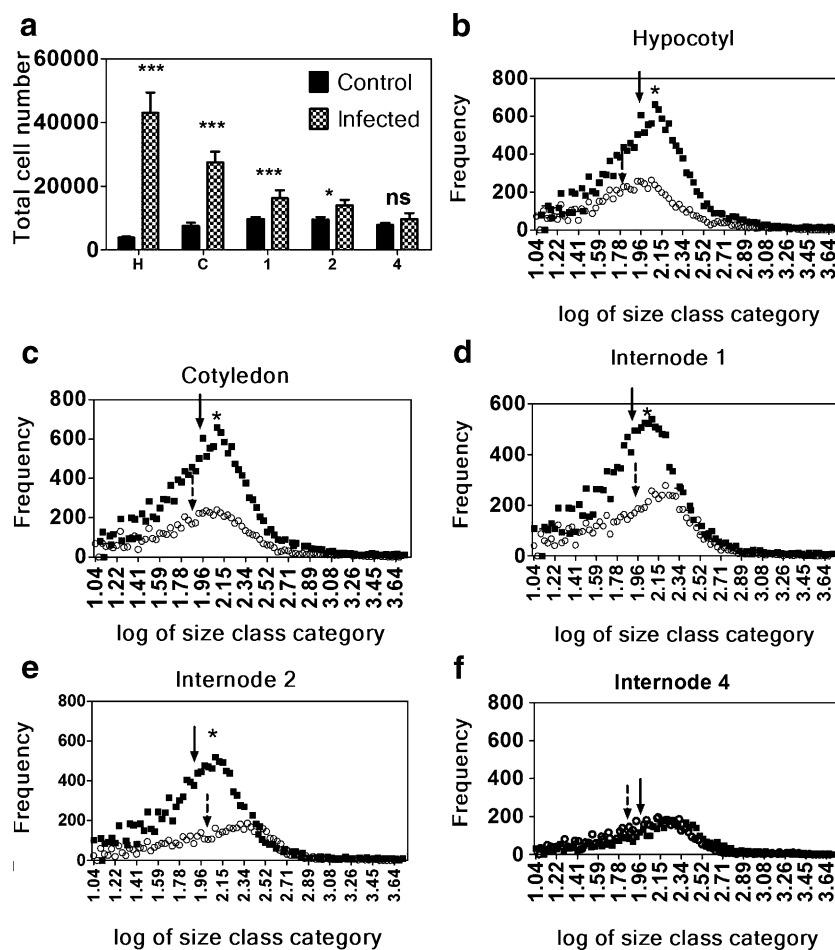
The symptoms observed on cacao and solanaceous showed very strong similarities (Fig. 1). The tomato variety Micro-Tom could switch to the necrotrophic phase whereas this phase was never observed on NC841-73. This could indicate that the tomato variety NC841-73 does not express the components necessary for the switch to occur.

In infected tomato plants, *M. perniciosa* induced the enlargement of stem tissues, particularly in phloem and

xylem regions (Figs. 3, 4 and 5). This is consistent with previous studies of cacao where xylem and phloem parenchyma tissues were significantly larger in infected plants [33]. Recent studies with susceptible and resistant cacao clones also showed that the radius of the xylem and phloem in the stems of susceptible plants was 50% larger than that of uninfected plants (Gramacho et al., personal communication). In tomato plants infected with *M. perniciosa*, the enlargement of the host's vascular tissue was associated with a higher cell number in the phloem and xylem of the infected tissues as compared to control tissues (Figs. 4a and 5a), suggesting that stem enlargement is caused by increased cell division in those tissues (hyperplasia).

The cells were larger in infected phloem and xylem tissues as shown by the significant upward shifts in the cell size distribution in the infected plants (Figs. 4 and 5). This result also indicates an increase in cell sizes in the infected plants (hypertrophy). To present knowledge, this is the first published account of the involvement of both hypertrophy and hyperplasia in the stem swelling caused by *M. perniciosa* in tomato. The major effect was observed in the hypocotyl and attenuated in the upper parts of the stem. Since inoculation occurred on the first emerging leaves, this

**Fig. 5** Cellular changes induced by *M. perniciosa* infection on tomato xylem. Cell number between infected and control plants at 5 different positions (C=cotyledons, H=hypocotyls, 1,2 and 4=first, second and fourth internode). Mean values were compared using a student t-test (a). Mean values were compared using a student t-test. Distributions of cell sizes using a logarithmic transformation (b–f). The distributions were compared using a Mann-Whitney test. The mean size values of the cell size for control (dashed arrows) and infected (solid arrows) are shown with an asterisk when differences are statistically significant



data shows that the cellular alterations caused by the fungus located around the inoculation point, decrease as a function of distance above the site of infection. Isolation of the fungus from infected plants has shown that fungal colonization is limited to sites below and above the inoculation point and does not reach the apical meristem (data not shown). This could explain the observed decrease in the disease phenotype at positions near the apical meristem.

The increase in stem diameter due to cell enlargement and cell division suggested that plant hormones might be involved in symptom development. Auxins play important roles in plant development and cell enlargement but can also be involved in disease development in many plant-pathogen interactions [23]. The best known system is crown gall formation caused by *Agrobacterium tumefaciens*, a pathogenic bacterium that induces overproduction of IAA (Indole Acetic Acid) in its hosts [41]. Likewise, *Pseudomonas syringae* also produces auxins during infection [16]. In *M. perniciosa*, the level of IAA oxydase, measured in liquid cultures, was high [26], suggesting that the fungus may be able to alter auxin concentrations by degrading it. In addition, hormone measurements in *M. perniciosa*-infected leaves showed that they contained 2.5

more IAA than uninfected leaves [25]. Recently, the whole genome of *M. perniciosa* has been sequenced, in which genes for auxin biosynthesis were identified. This suggests that the fungus may also be able to synthesize the hormone [31]. Moreover, auxins have been shown to induce xylogenesis (formation of xylem tissue) [46], which is one of the most noticeable changes observed during infection by *M. perniciosa* (Fig. 3). Other changes include the activation of axillary buds and the reduction of root biomass, which were also observed in tomato and pepper plants. This activation could be caused by the disruption of the natural auxin gradient, which regulates apical dominance in plants [29]. The result from transgenic plants carrying GUS under the control of the DR5 inducible promoter suggests altered auxin levels in the infected plants. The question of whether the fungus produces auxins or induces auxin biosynthesis remains to be investigated.

In infected tomato tissues, *M. perniciosa* intercellular biotrophic hyphae were found associated with calcium oxalate crystals (Fig. 6). Since production of these crystals occurred in the apoplastic space and not in specialized plant cells (idioblasts), and were often associated with fungal hyphae [11], these crystals are likely originated from the

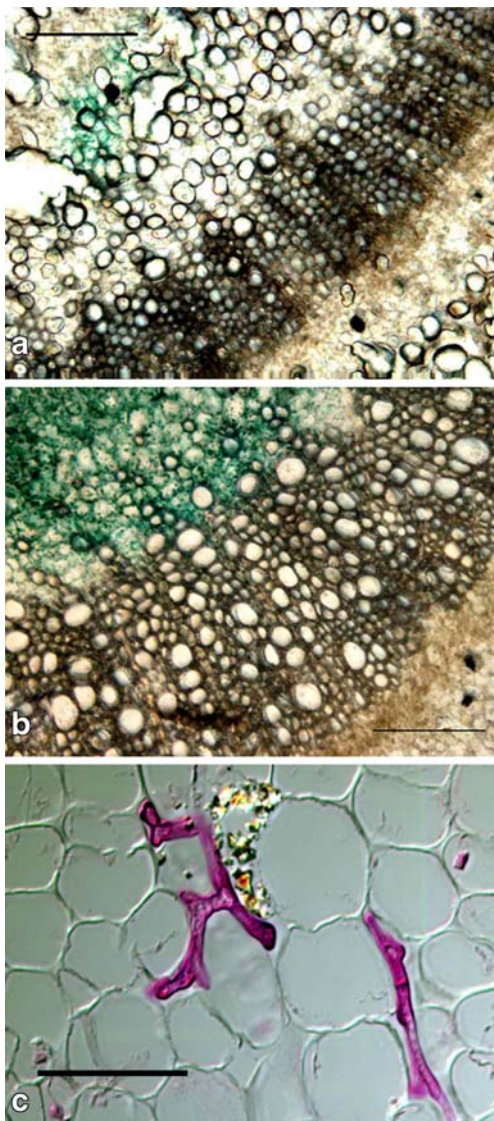


**Fig. 6** Fungal colonization on infected tomato tissue and auxin localization. **a** Presence of GUS expression on control plant **(b)** GUS expression on infected plant. Plants were sectioned six weeks after inoculation and stained for GUS following the standard GUS staining protocol [24]. Bar=100 $\mu$ m **(c)** Biotrophic fungal hyphae growing in the phloem parenchyma cells near calcium oxalate clusters. Bar=50 $\mu$ m

fungus. Consistent with this observation, as compared to non-inoculated control plants, increased calcium oxalate crystals was observed in susceptible genotypes of cacao infected with *M. perniciosa* [7]. A sharp decrease in crystals was also observed during the rapid necrosis leading to the necrotrophic phase, suggesting a role of oxalate in programmed cell death [7]. Crystals of calcium oxalate were also found associated with saprophytic hypha of *M. perniciosa* growing on a glass slide [10]. Moreover, the oxaloacetate acetylhydrolase gene (*oah*), essential for oxalic acid biosynthesis, was upregulated in biotrophic mycelium grown on cocoa meristem extract [39].

The data presented here clearly demonstrates that the S-biotype of *M. perniciosa* is pathogenic to *S. lycopersicum* (tomato) and *Capsicum annuum* (pepper) and produces symptoms similar to those of the witches' broom disease, such as activation of axillary buds, cell enlargement and multiplication, oxalate crystal production and switch to a necrotrophic phase (Fig. 1). The fact that in some tomato varieties *M. perniciosa* does not present a transition to the necrotrophic phase could be studied further since transferring this trait to cacao could consist in a very efficient control strategy.

A close observation of the interaction between the S-biotype of *M. perniciosa* and the solanaceous plants provided an insight into pathogenesis mechanisms. This insight is potentially useful for developing methods to control the disease in cacao. For example, tomato can potentially be used to test the efficacy of various control strategies such as biological control agents, transgenic expression of pathogenesis-related proteins (e.g. chitinase), and novel target-based chemicals. The feasibility of large scale experiments and the availability of various types of materials for genetic mapping in tomato plants is an advantage that can shorten the time necessary to elucidate the mechanisms of the *M. perniciosa* infection process. The information extracted from the infection biology of *M. perniciosa* in tomato plants could be very useful for understanding complex mechanisms for finding target-based control agents applicable to cacao in control programs.

## Methods

### *Moniliophthora perniciosa* Isolates

All isolates of *M. perniciosa* used in this study (Table 1) are maintained in a solution of MES 0.01 M and 16% glycerol in liquid nitrogen as part of the *Moniliophthora* collection at the Pennsylvania State University (APHIS permit # 72545). For the S-biotype, basidiocarps were produced from the monosporadic strain 73-6-01, which was collected from infected *Solanum paniculatum* near the Mars Center for Cocoa Science in Bahia (Brazil). An infected cacao plant in Bahia was the source of strain 73SP16 (C-biotype) that was subsequently single spored. Spores or mycelium were plated on Potato Dextrose Agar (Difco) and grown at 25°C for 1 month for genomic DNA extraction.

### Phylogenetic Analysis

To determine the phylogenetic relationships between the S and C biotypes, nine isolates from the Penn State Collection and 18 isolates from the Genebank were analyzed (Table 1).

**Table 1** Fungal isolates included in the phylogenetic analysis of the ITS sequence

Isolate	Host	Original material	Geographical location	ITS Genebank accession number.	Species
73-63	<i>S.paniculatum</i>	Green broom	Camaca-Serra Boa, BA, Brazil	EU047931	<i>M. pernicioso</i>
92-10-7	<i>S.rugorosum</i>	n/a	Manaus, AM, Brazil	EU047930	<i>M. pernicioso</i>
1189G	<i>T.cacao</i>	Green Broom	Itanhem Sombra da Tarde, BA, Brazil	EU047932	<i>M. pernicioso</i>
1441G	<i>T.cacao</i>	Green Broom	CEPEC, BA, Brazil	EU047933	<i>M. pernicioso</i>
1480	<i>T.cacao</i>	Green Broom	n/a	EU047934	<i>M. pernicioso</i>
KG06	<i>S.paniculatum</i>	Green Broom	Vale do Jequitinhonha, BA, Brazil	EU047935	<i>M. pernicioso</i>
73-6-01	<i>S.paniculatum</i>	n/a	Itajuípe Almirante, BA, Brazil	EU047929	<i>M. pernicioso</i>
1188	<i>T.cacao</i>	n/a	n/a	EU047936	<i>M. pernicioso</i>
M.Gflorum	<i>T. grandiflorum</i>	n/a	n/a, Ecuador	EU047937	<i>M. roreri</i>
CANG/1	<i>T.cacao</i>	Basidioma in culture	Canavieiras, BA, Brazil	AY317131[G]	<i>M. pernicioso</i>
UB/21998	<i>T.cacao</i>	Basidioma in culture	Ilheus, BA, Brazil	AY317132[G]	<i>M. pernicioso</i>
BE12/18	<i>T.cacao</i>	Basidioma in culture	Belem, Para, Brazil	AY317133[G]	<i>M. pernicioso</i>
UB/2021	<i>T.cacao</i>	Basidioma in culture	Manaus, AM, Brazil	AY317134[G]	<i>M. pernicioso</i>
UB/2027	<i>T.cacao</i>	Basidioma in culture	Ouro Preto, RO, Brazil	AY317135[G]	<i>M. pernicioso</i>
UB/2041	<i>S.lycocarpum</i>	Basidiome/necrotic broom	Lavras, MG, Brazil	AY317136[G]	<i>M. pernicioso</i>
UB/2054	<i>T.grandiflorum</i>	Basidiome/necrotic broom	Manaus, AM, Brazil	AY317127[G]	<i>M. pernicioso</i>
FA617	<i>T. grandiflorum</i>	Basidiome/necrotic broom	Itajuípe Almirante, BA, Brazil	AY317129[G]	<i>M. pernicioso</i>
FA619	<i>S.paniculatum</i>	Basidiome/necrotic broom	Itajuípe Almirante, BA, Brazil	AY317130[G]	<i>M. pernicioso</i>
n/a	<i>T.grandiflorum</i>	Vegetative Dikaryotic Mycelium	n/a, Brazil	AY216468[G]	<i>M. pernicioso</i>
n/a	<i>T.subincantum</i>	Vegetative Dikaryotic Mycelium	na/na, Brazil	AY216469[G]	<i>M. pernicioso</i>
CP-37	<i>S. paniculatum</i>	Vegetative Dikaryotic Mycelium	n/a, BA, Brazil	AY216470[G]	<i>M. pernicioso</i>
n/a	<i>S. paniculatum</i>	Vegetative Dikaryotic Mycelium	n/a, Brazil	AY176316[G]	<i>M. pernicioso</i>
CP-83	<i>Herrania sp.</i>	Vegetative Dikaryotic Mycelium	n/a, BA, Brazil	AY216471[G]	<i>M. pernicioso</i>
CP-104	<i>C. frutescens</i>	Vegetative Dikaryotic Mycelium	n/a, Bahia, Brazil	AY216472[G]	<i>M. pernicioso</i>
RNBP1	<i>T.cacao</i>	Vegetative Dikaryotic Mycelium	Quillabamba, Peru	AF335590[G]	<i>M. pernicioso</i>
n/a	n/a	n/a	n/a	AY230255[G]	<i>M.roreri var. gileri</i>
strainCBB-361	n/a	Vegetative Dikaryotic Mycelium	n/a	AY216476[G]	<i>Marasmius sp.</i>

n/a not available

Genomic DNA was extracted from vegetative dikaryotic mycelium as previously described [47]. The region spanning the internal transcribed spacers of ribosomal RNA encoding genes ITS1, 5.8S RNA, and ITS2 was amplified from each strain by PCR using the universal primer pair ITS4 (TCCTCCGCTTATTGATATGC) and ITS5 (GGAAGTAAAAGTCGTAACAAGG). Amplification was verified on a 0.8% agarose gel, and PCR products were purified using Qiagen DNA purification columns (Qiagen cat # 28104). PCR products were sequenced using an ABI Hitachi 3730XL DNA analyzer (Applied Biosystems). Eighteen additional ITS sequences of *M. pernicioso*, generated in a previous study [9], were obtained from Genebank. The resulting 27 ITS sequences (Table 1) were aligned using the Clustal W algorithm with MEGA 3.1 software [27]. A neighbor-joining tree was constructed with

MEGA 3.1 with statistical support for branch topology tested by bootstrap analysis derived from 1000 replicates. Since a previous report indicates that *M. roreri* is closely related to *M. pernicioso* [2], one *M. roreri* isolate collected from *Theobroma grandiflorum* (Mgflorum) and one *M. roreri* var. *gileri* type from *T.cacao* were included in the analysis. Additionally, strain CBB361 of *Marasmius* spp. (both *M. pernicioso* and *M. roreri* belong to the Marasmiaceae) was used as the outgroup to root the tree.

#### Inoculum Production

Basidiocarps were produced from S- and C-biotype strains using the bran-vermiculite *in vitro* method [18, 32]. “Cookies” of the bran cultures were hung in a 40 gallon fish tank and maintained at 25°C with alternations between

a 10-hr period at 100% humidity and a 14-hr period at 50% humidity. Water mist from an ultra-sonic humidifier supplied humidity. After 2 to 3 months, basidiocarps were harvested and the inoculum was collected by attaching the mushroom caps onto Petri-dish lids with petroleum jelly and placing them over flasks containing 5–10 ml of MES 0.01 M, 16% glycerol buffer. The resulting spore suspension was then frozen in liquid nitrogen until used.

#### Plant Material and Sterilization

Seeds of *S. lycopersicum* (cvs. New Yorker, NC841.73 and Micro-Tom), and *Capsicum annum* (cv. Tequila Sunrise) were surface-sterilized with 2% NaOCl (commercial bleach) for 20 min and washed 3 times with sterile distilled water for 2 min each time. Seeds were pre-germinated in the dark over moist sterile filter paper for 3–4 days at 25°C. After germination, seeds were sown in 100 ml pots containing Scotts® ready-earth soil and grown at 25°C with 16:8 h light-dark periods at 60% humidity. Seedlings of cacao (cv. Comum) were sown and kept in a greenhouse under the same conditions. The plants were fertilized once a week with 1/10 Hoagland solution (160 ppm).

#### Plant Infection

The method of [45] was used to infect plants. Using a hemacytometer, inoculum concentration was adjusted to  $6 \times 10^5$  spores per ml with a solution of 0.01 M MES and 0.25 % agar. A 10 µl drop of inoculum was placed on the youngest emerging leaf using a micro-pipette. The plants were then placed in the dark for 48 h in a dew chamber (Percival # Model E-54U DL) at temperatures ranging from 25–27°C and 100% humidity. Under these conditions small water droplets accumulated on the leaves. The rate of spore germination was evaluated before and after plant inoculation by plating 10 µl inoculum on a water agar plate that was incubated under the same conditions as the inoculated plants. The plants were subsequently transferred to a growth chamber set at 25°C with a relative humidity of 60% and a 16:8 h light: dark period for 2–3 months. Images of infected plants were taken every week using a C-4000 zoom digital camera (Olympus) to record morphological changes.

#### Morphometric Analysis

To investigate the cellular basis of stem swelling, the first emerging leaf of ten day-old tomato plants (NC841.73) was inoculated in a completely randomized experiment with 10 replicates per treatment. Among the controls and the treated plants, 3 plants were randomly selected and stem samples (five 1-cm long sections) were collected 8 weeks post

inoculation. The middle of the hypocotyl (H), the cotyledonary node (C) and internodes 1, 2 and 4 were used as reference points. Stem sections were fixed in formaldehyde acetic alcohol (50% ethanol, 5% glacial acetic acid, 10% formalin, and 35% water) for 24 h at room temperature. Fixed samples were dehydrated by treating them with a series of ethanol solutions: 50% (1 h), 70% (15 min), 95% (8.5 h), and 100% (1.5 h). Paraffin embedding was conducted using a Shandon Citadel 2000 paraffin processor (Thermo Scientific). Five to ten µm cross-sections were generated using a Leica 2000 paraffin microtome (Leica Microsystems) and placed onto positively charged slides (Thermo Scientific Shandon, NC9180670). Sections were cleared with xylene and the cell walls and fungal hyphae were stained with calcofluor (0.01%). Alternatively, sections were stained with Pianezze IIIB to specifically stain fungal hyphae and observations were conducted via bright-field microscopy as previously described [17, 48]. Fungal hyphae stained with Pianezze III B [17] appeared pink when observed using difference interference contrast (DIC). A microscope connected to an AxioCam MRm digital camera (Zeiss) was used to collect the images. The presence of calcium oxalate crystals was observed under polarized light and by staining with silver nitrate as previously described [28].

To measure the total area of whole sections, mosaics of 10x images were taken using a Olympus BX60 microscope with a motorized stage, under UV light and taken with a Hamamatsu cooled digital camera (ORCA 100, Model #C4742-95). For precise cell measurements, an inverted Axiovert 200 Zeiss microscope (Zeiss) with UV filter was used.

Individual images were processed manually using a tablet PC to correct for image artifacts and measured using the “analyze particles” function on Image J V. 1.38X [1]. The total area of each tissue type, cell size distribution, cell density (number of cells per unit area) and total number of cells (cell density X total area) were quantified and compared between infected and control plants. In total, this analysis involved six biological replicates for each of the five positions studied. Cell numbers between control and infected plants, and cell size distribution (logarithmic transformations) were compared using a Student t-test and a Mann-Whitney test respectively using the statistical package R [22].

#### Genetic Transformation of Tomato Plants with the GUS Gene Under the Control of the DR5 Auxin Inducible Promoter

The DR5 construct is a synthetic promoter inducible by auxin and consists of 7 tandem repeats (TGTCTC) spaced by 5 bp [21]. *Agrobacterium* mediated transformation

(ATMT) of tomato (var. Micro-Tom) was performed at the University of California Davis Plant Transformation Facilities. Transgenic plants expressing GUS were grown and infected as described above. Six weeks after inoculation, plants were sectioned at the sites of swelling and stained for GUS activity as previously described [24].

**Acknowledgements** We would like to thank Dr. Majid Foolad (The Pennsylvania State University, Department of Horticulture) for providing tomato seeds (NC841.73). Thanks to Dr Paul Backman for useful comments and for providing lab space to work with the pathogen under containment conditions. Thanks also to Ruth Haldeman, Susan Mogargee and Elaine Kunze for technical assistance with microscopy and to Dr. Sook-Young Park for her technical assistance with molecular techniques. This work was supported in part by the American Cocoa Research Institute Endowed Program in the Molecular Biology of Cocoa, by Grants to M.J.G. from the World Cocoa Foundation and the United States Department of Agriculture Office of International Research Programs, and by support from the Departments of Plant Pathology and Horticulture, Agricultural Experiment Station of The Pennsylvania State University (CRIS 3550).

## References

- Abramoff MD, Magelhaes PJ, Ram SJ (2004) Image processing with imageJ. *Biophotonics* 11(7):36–42
- Aime MC, Phillips-Mora W (2005) The causal agents of witches' broom and frosty pod rot of cacao (chocolate, *Theobroma cacao*) form a new lineage of Marasmiaceae. *Mycologia* 97(5):1012–1022
- Anderbrhan T, Furtak DB (1994) Random amplified polymorphic DNA (RAPD) analysis of *Crinipellis perniciosa* isolates from different hosts. *Plant Pathol* 43:1020–1027
- Bastos CN, Anderbrhan T, Almeida LC (1988) Morphological and pathological comparison of *Crinipellis perniciosa* isolates. *Fitopatol bras* 13(3):2002–2006
- Bastos CN, Evans HC (1985) A new pathotype of *Crinipellis perniciosa* (Witches' broom disease) on solanaceous hosts. *Plant Pathol* 34:306–312
- Bowers JH, Bailey BA, Hebban PK, S.Sanogo, and Lumsden RD (2001) The impact of plant diseases on world chocolate production. In APS net features. Available via <http://www.apsnet.org/online/feature/cacao/>
- Ceita GO, Macedo JNA, Santos TB, Alemanno L, Gesteira AS, Micheli F, Mariano AC, Gramacho KP, Silva DC, Meinhardt L, Mazzafera P, Guimaraes Pereira GA, Cascardo JCM (2007) Involvement of calcium oxalate degradation during programmed cell death in *Theobroma cacao* tissues triggered by the hemibiotrophic fungus *Moniliophthora perniciosa*. *Plant Sci* 173:106–117
- Cronshaw DK, Evans HC (1978) Witches' broom disease of cocoa (*Crinipellis perniciosa*) in Ecuador. II- Methods of infection. *Ann Appl Biol* 89:193–200
- de Arruda MCC, Sepulveda GF, Miller RNG, Ferreira MASV, Santiago DVR, Resende MLV, Dianese JC, Felipe MSS (2005) *Crinipellis brasiliensis*, a new species based on morphological and molecular data. *Mycologia* 97(6):1348–1361
- do Rio MCS, de Oliveira BV, de Tomazella DPT, da Silva JAF, Pereira GAG (2008) Production of calcium oxalate crystals by the basidiomycete *Moniliophthora perniciosa*, the causal agent of Witches' Broom disease of cacao. *Curr Microbiol* 56(4):363–370
- Dutton MV, Evans CS (1996) Oxalate production by fungi: its role in pathogenicity and ecology in the soil environment. *Can J Microbiol* 42(9):881–895
- Evans HC (1978) Witches' broom disease of cocoa (*Crinipellis perniciosa*) in Ecuador. I- The fungus. *Ann Appl Biol* 89:185–192
- Evans HC (1980) Pleomorphism in *Crinipellis perniciosa*, causal agent of witches' broom disease of cocoa. *Trans Br Mycol Soc* 74(3):515–523
- Evans HC, Barreto RW (1996) *Crinipellis perniciosa*: a much investigated but little understood fungus. *Mycologist* 10(2):58–61
- Frias GA, Purdy LH (1991) Infection biology of *Crinipellis perniciosa* on vegetative flushes of cacao. *Plant Dis* 75:552–556
- Glickmann E, Gardan L, Jacquet S, Hussain S, Elasmri M, Petit A, Dessaux Y (1998) Auxin production is a common feature of most pathovars of *Pseudomonas syringae*. *Mol Plant Microbe Interact* 11(2):156–162
- Gramacho KP (1999) Disease resistance and pathogenic variability in the fusiform rust-slash pine pathosystem. Dissertation, University of Florida
- Griffith GW, Hedger JN (1993) A novel method for producing basidiocarps of the cocoa pathogen *Crinipellis perniciosa* using a bran-vermiculite medium. *Neth J Plant Pathol* 99:227–230
- Griffith GW, Hedger JN (1994) Spatial distribution of mycelia of the liana (L-) biotype of the garic *Crinipellis perniciosa* (Stahel) Singer in tropical forest. *New Phytol* 127:243–259
- Griffith GW, Nicholson J, Negnninger A, Birch RN, Hedger JN (2003) Witches' brooms and frosty pods: two major pathogens of cacao. *New Zeal J Bot* 41:423–435
- Hagen G, Guilfoyle T (2002) Auxin-responsive gene expression: genes, promoters and regulatory factors. *Plant Mol Biol* 49:373–385
- Ihaka R, Gentleman R (1996) R: a language for data analysis and graphics. *J Comput Graph Stat* 5(3):299–314
- Jameson PE (2000) Cytokinins and auxins in plant-pathogen interactions—An overview. *Plant Growth Regul* 32(2–3):369–380
- Jefferson RA, Kavanagh TA, Bevan MW (1987) Gus fusions—beta-glucuronidase as a sensitive and versatile gene fusion marker in higher-plants. *Embo J* 6(13):3901–3907
- Kilaru A, Bailey BA, Hasenstein KH (2007) *Moniliophthora perniciosa* produces hormones and alters endogenous auxin and salicylic acid in infected cocoa leaves. *FEMS Microbiol Lett* 274(2):238–244
- Krupasagar V, Sequeira L (1969) Auxin destruction by *Marasmius pernicius*. *Am J Bot* 56(4):390–397
- Kumar S, Tamura K, Nei M (2004) MEGA3: integrated software for molecular evolutionary genetics analysis and sequence alignment. *Brief Bioinform* 5:150–163
- Kurrein F, Green G, Rowles S (1975) Localized deposition of calcium oxalate around a pulmonary *Aspergillus niger* fungus ball. *Am J Clin Pathol* 64:556–563
- Leyser O (2003) Regulation of shoot branching by auxin. *Trends Plant Sci* 8(11):541–545
- Meinhardt LW, Rincones J, Bailey BA, Aime MC, Griffith GW, Zhang DP, Pereira GAG (2008) *Moniliophthora perniciosa*, the causal agent of witches' broom disease of cacao: what's new from this old foe? *Mol Plant Pathol* 9(5):577–588
- Mondego JMC et al. (2008) A genome survey of *Moniliophthora perniciosa* gives new insights into witches' broom disease of cacao. *BMC Genomics*, 9
- Niella GR, Resende MI, Castro HA, Silva LHCP, Carvalho JA (1999) Aperfeiçoamento da metodologia de producao artificial de basidiocarpos de *Crinipellis perniciosa*. *Fitopatol bras* 23:523–527
- Orchard J, Collin HA, Hardwick K, Isaac S (1994) Changes in morphology and measurement of cytokinin levels during the development of witches' broom on cocoa. *Plant Pathol* 43:65–72

34. Pires ABL, Gramacho KP, Silva DC, Goes-Neto A, Silva MM, Muniz-Sobrinho JS, Porto RF, Villela-Dias C, Brendel M, Cascardo JCM, Pereira GAG (2009) Early development of *Moniliophthora perniciosa* basidiomata and developmentally regulated genes. *BMC Microbiol* 9:18
35. Ploetz R, Shnell RJ, Ying Z, Zheng Q, Olano CT, Matamayor JC, Johnson ES (2005) Analysis of molecular diversity in *Crinipellis perniciosa* with AFLP markers. *Eur J Plant Pathol* 111:317–326
36. Purdy LH, Schmidt RA (1996) Status of cacao witches broom: biology, epidemiology, and management. *Ann Rev Phyto* 34:573–594
37. Radzali BM, Hamish AC, Issac S, Hardwick K (1996) Effects of the fungus *Crinipellis perniciosa*, causal agent of witches' broom disease, on cell and tissue cultures of cocoa (*Theobroma cacao* L.). *Plant Pathol* 45:145–154
38. Rincones J, Mazotti GD, Griffith GW, Pomela A, Figueira A, Leal GA, Queiroz MV, Pereira JF, Azevedo RA, Pereira GAG, Meinhardt LW (2006) Genetic variability and chromosome-length polymorphisms of the witches' broom pathogen *Crinipellis perniciosa* from various parts in South America. *Mycol Res* 110:821–832
39. Rincones J, Scarpari LM, Carazzolle MF, Mondego JMC, Formighieri EF, Barau JG, Costa GGL, Carraro DM, Brentani HP, Vilas-Boas LA, de Oliveira BV, Sabha M, Dias R, Jim C, Azevedo RA, Meinhardt LW, Pereira GAG (2008) Differential gene expression between the biotrophic-like and saprotrophic mycelia of the witches' broom pathogen *Moniliophthora perniciosa*. *Mol Plant Microbe Interact* 21(7):891–908
40. Scarpari LM, Meinhardt LW, Mazzafera P, Pomella AWV, Schiavinato MA, Cascardo JCM, Pereira GAG (2005) Biochemical changes during the development of witches' broom: the most important disease of cocoa in Brazil caused by *Crinipellis perniciosa*. *J Exp Bot* 56(413):865–877
41. Schwalm K, Aloni R, Langhans M, Heller MW, Stich S, Ullrich CI (2003) Flavonoid-related regulation of auxin accumulation in *Agrobacterium tumefaciens*-induced plant tumors. *Planta* 218:163–178
42. Silva SDVM, Luz EDMN, Almeida LC, Gramacho KP, Bezerra JL (2002) Redescricao da sintomatologia causada por *Crinipellis perniciosa* em cacauero. *Agrotropica* 14(1):1–10
43. Sreenivasan TN, Dabydeen S (1989) Modes of penetration of young cocoa leaves by *Crinipellis perniciosa*. *Plant Dis* 73:478–481
44. Stahel G (1919) Contribution to the knowledge of witchbroom disease. *Trop Agr* 4(6):167–176
45. Surujdeo S, Umaharan P, Butler DR, Sreenivasan TN (2003) An optimized screening method for identifying levels of resistance to *Crinipellis perniciosa* in cocoa (*Theobroma cacao*). *Plant Pathol* 52:464–475
46. Taiz L, Zeiger E (1998) *Plant physiology*. Sinauer Associates, Inc., Sunderland
47. Thomson D, Henry RJ (1993) Single step protocol for preparation of plant tissue for analysis by PCR. *Biotechniques* 19:394–397
48. Vaughan RE (1914) A method for the differential staining of fungus and host cells. *Ann Mo Bot Gard* 1:241–242